ELSEVIER

S0032-3861(96)00386-2

Polymer Vol. 37 No. 24, pp. 5421–5431, 1996

0032-3861/96/$15.00 + 0.00

Melt rheological behaviour of short pineapple fibre reinforced low density polyethylene composites

Jayamol George
School of Chemical Sciences, Mahatma Gandhi University, Priyadarshini Hills PO, Kottayam, Kerala – 686 560, India

and R. Janardhan and J. S. Anand
Central Institute of Plastics Engineering and Technology, Guindy, Madras – 600 032, India

and S. S. Bhagawan
Propellent Engineering Division, Vikram Sarabhai Space Centre, Thiruvananthapuram, Kerala – 696 022, India

and Sabu Thomas*
School of Chemical Sciences, Mahatma Gandhi University, Priyadarshini Hills PO, Kottayam, Kerala – 686 560, India
(Received 19 July 1995; revised 8 January 1996)

The melt rheological behaviour of short pineapple fibre reinforced low density polyethylene composite has been studied using a capillary rheometer. The influence of fibre loading, fibre length, and fibre treatment on the rheology of composites was investigated. Studies were carried out in the temperature range of 125 to 145°C and shear rate of 016.4 to 5468 s^{-1}. The melt viscosity was found to be increased with fibre loading. Various chemical treatments were made to improve fibre–matrix interfacial adhesion. Treatments based on poly(methylene)–poly(phenyl)isocyanate (PMPPIC), silane and peroxide increased the viscosity of the system due to high fibre–matrix interfacial interaction. Viscosity of the system decreased with increase of temperature. However, in peroxide treated composites viscosity is increased due to the crosslinking of composite at higher temperature. The fibre breakage during extrusion was analysed using optical microscopy. The morphology of the extrudates has been studied by optical and scanning electron microscopies. Master curves were generated using modified viscosity and shear rate functions that contain melt flow index as a parameter. Copyright © 1996 Elsevier Science Ltd.

(Keywords: melt rheology; pineapple fibre; composites)

INTRODUCTION

In recent years, cellulose fibre reinforced thermoplastic composites have found wide use in structural and non-structural applications because of their superior mechanical properties. The choice of suitable processing conditions is guided mainly by the rheological behaviour of composites. A number of investigations on the rheological behaviour of short fibre reinforced thermoplastics and elastomers have been reported[1–4]. Incorporation of fillers in thermoplastics will increase the melt viscosity which may result in unusual rheological effects. Studies on the rheological behaviour of filled thermoplastics and its application in injection moulding have been reported. Gupta and Purwar[5] reported on the effect of glass fibres on the rheological behaviour of thermoplastics. Molden[6] developed a simple geometrical theory and showed that convergent flow is more effective than shear flow in aligning fibres. Subsequent shear flow along the die can cover a significant misalignment of fibres and the fibre orientation at the exit of the die is a function of the flow rate and L/D ratio. Crowson *et al.*[7,8] reported in detail the flow behaviour of short glass fibre reinforced thermoplastics during injection moulding. Composite viscosity is considerably influenced by fibre loading and fibre length at lower shear rate than at higher shear rate. The rheological behaviour of short jute fibre composites has been studied by Murthy *et al.*[9]. Melt flow behaviours or short sisal fibre in different polymer systems were reported by Thomas and co-workers[10,11].

Recently short pineapple leaf fibre (PALF) was used as a good reinforcing material for low density polyethylene (LDPE)[12–14]. The short-term and long-term mechanical properties and viscoelastic behaviour of these composites were studied in detail[12–14]. The present paper deals with the rheological characteristics of short PALF reinforced LDPE composites. The effects of fibre loading, fibre length, chemical treatments and temperature on melt

* To whom correspondence should be addressed

viscosity have been investigated. The experimental viscosity values were compared with theoretical predictions. Shear stress–temperature superposition was done to predict the melt viscosities of the composite materials. Finally, master curves were generated using capillary and melt flow index data.

EXPERIMENTAL

Low density polyethylene (16 MA 400) was obtained from Indian Petro Chemical Corporation Ltd, Vadodara. Pineapple leaf fibre (*Ananus cosomus*) was supplied by South India Textile Research Association, Coimbatore. The physical and mechanical properties of LDPE and PALF are reported elsewhere[12].

Poly(methylene)–poly(phenyl)isocyanate (PMPPIC), supplied by Poly Sciences, USA, and vinyl tri-2(ethoxy methoxy silane) (Silane A-172), supplied by Union Carbide Co., Montreal, Canada, were used as coupling agents.

Benzoyl peroxide (BPO), dicumyl peroxide (DCP) and NaOH (Reagent grade) were used as surface modifiers to improve the adhesion between fibre and matrix.

Fibre treatment

Alkali treatment. Fibres were immersed in NaOH (0.5%) solution for half an hour. Later these were washed several times with cold water and finally with acidified water (HCl 0.1 N). These fibres were dried in an air oven at 60°C for 24 h.

Silane treatment (Silane A-172). A mixture of oven dried fibres, carbon tetrachloride, dicumyl peroxide (2 wt% of fibre) and silane (4 wt% of fibre) was heated under reflux for 2 h. Finally, the mixture was filtered and dried.

Isocyanate treatment (PMPPIC). Fibres were dipped in toluene solution containing PMPPIC (5 wt% of fibre) for half an hour at 50°C. The fibres were then decanted and dried in an air oven at 70°C for 2 h. Later these were mixed with polyethylene using toluene as the solvent containing PMPPIC (6 wt% of fibre) at a temperature of 120°C.

Peroxide treatment. Benzoyl peroxide (1 wt% of polymer) and dicumyl peroxide (0.5 wt% of polymer) were added to a melt of polyethylene before being mixed with fibres.

Preparation of composites

Composites were prepared by solution mixing technique. Fibres were added to a viscous slurry of polyethylene which was prepared by adding toluene to a melt of polyethylene. After thorough mixing, the composite was transferred into a tray, and solvent was removed using a vacuum oven. The solvent-free composites were charged into a ram type hand injection moulding machine at a temperature of 125°C and material was injection moulded in the form of rods.

Rheological measurements

The melt rheological measurements were carried out using an Instron Capillary Rheometer model 3211 at different plunger speeds of 0.06 to 20 mm min^{-1}. The capillary used was made of tungsten carbide with length to diameter (L/D) ratio of 33.42 and an angle of entry of 90°C. The sample was placed inside the barrel of the extrusion assembly and forced down into the capillary with a plunger. After a residence time of 5 min, the melt was extruded through the capillary at predetermined plunger speeds. The initial position of the plunger was kept constant in all experiments and shear viscosities at different shear rates were obtained from a single charge of material. The measurements were carried out at three different temperatures, namely 125, 135 and 145°C.

The shear stress at each plunger speed is obtained from the equation:

$$\tau = \frac{F}{4A_p(l_c/d_c)} \tag{1}$$

where F is the force on the plunger, A_p is the cross-sectional area of the plunger, and l_c and d_c are the length and diameter of capillary. The shear rate at the wall was determined using the equation:

$$\dot{\gamma} = \frac{(3n' + 1)}{4n'} \frac{32Q}{\pi d_c^3} \tag{2}$$

where Q is the volumetric flow rate which is given by:

$$Q = \frac{Vxh}{60} \frac{\pi d_b^2}{4} \tag{3}$$

where Vxh is the plunger speed (mm min^{-1}) and d_b is the diameter of the barrel.

The factor $3n' + 1/4n'$ is the Rabinowitch correction applied to calculate the shear rate at the wall. The flow behaviour index (n') given by

$$n' = \frac{d(\log \tau)}{d(\log \dot{\gamma})} \tag{4}$$

is obtained by the regression analysis of the plot of log τ *versus* log $\dot{\gamma}$.

Bagley's correction[15] for the pressure drops at the capillary entrance was not applied because this correction factor becomes negligible for capillaries with high l/d ratios. The viscosity (η) is calculated using the equation:

$$\eta = \frac{\tau}{\dot{\gamma}} \tag{5}$$

The melt flow index (MFI) was determined using a Davenport Melt Flow Indexer with 21.6 kg load. The measurements were made at a temperature of 145°C.

Extrudate morphology

The distortion and surface characteristics of the extrudate were studied using optical and electron microscopies. The extrudate were fractured under liquid nitrogen and the morphology of the extrudate cross-section was studied using a scanning electron microscope (JEOL JSM 35 C model).

Fibre breakage analysis

Fibre breakage during extrusion at different shear rates was analysed by dissolving the polyethylene from the extrudate and measuring the fibre length using a travelling microscope. Polydispersity index was calculated from fibre length distribution.

RESULTS AND DISCUSSION

Effect of shear rate and fibre loading on viscosity

The dependence of fibre loading and shear rate on melt viscosity is shown in *Figure 1*. The curves are typical of pseudoplastic materials. It is clear that viscosity of the system increases with fibre loading. The increase in viscosity is more predominant at lower shear rate than at higher shear rates. In general, the pseudoplastic behaviour of polymeric systems can be explained in two ways[4]. (a) If a system of asymmetric particles, which are initially randomly dispersed, is subjected to shear, the particles tend to align themselves with the major axis, in the direction of shear, thus reducing the viscosity. The degree of alignment is a function of the deformation rate. At low shear rates, there is only a slight departure from randomness but at higher shear rates, particles are almost completely oriented. (b) In highly solvated systems, when chemical interaction among polymer particles exists, with increase of shear rate, the solvated layers may be sheared away resulting in decreased viscosity.

The fibre-filled systems exhibit higher viscosity than the pure polymer at all shear rates. In filled system, fibres will perturb the normal flow of polymer and hinder the mobility of chain segments in flow. Crowson *et al.*[7,8] reported the effect of the converging flow in the die entrance region which will result in high fibre alignment. This will occur when a fluid passes from a wide to a narrow cross-section. At low shear rate, fibres are disoriented. The probability of fibre–fibre collision is much higher for misaligned fibres. This collision increases with fibre loading and as a result viscosity increases. But as the shear rate increases, most of the shearing of fibres takes place closer to the tube wall and the fibres will align strongly along the tube axis. Therefore the probability of fibre–fibre collision is much lower and so the increase in viscosity with fibre content is less at high shear rates. Goldsmith and Mason[16] have also observed radial migration of filler particles towards the capillary axis during shear flow. If this occurs during the flow of fibre-filled thermoplastics, the region where most of the shear takes place may be virtually fibre free. This could be a reason for the small dependence of viscosity on fibre concentration at high shear rates. Wu[17] also reported that migration occurs during the extrusion of glass fibre filled poly(ethylene terephthalate). The very close viscosity values at high shear rates, for filled and unfilled thermoplastics, is an important factor in explaining the successful exploitation of these materials in injection moulding technology, since very little additional power will be required to mould the filled materials (*Figure 1*).

Effect of shear stress and fibre loading on viscosity

The dependence of viscosity of PALF–LDPE composites on shear stress for different fibre loading is shown in *Figure 2*. It is observed that in all cases the viscosity of all the systems decreased with an increase in shear stress due to the orientation of the fibre and polymer molecules in the direction of extrusion. It may be noted that no yield stress is exhibited by PALF–LDPE composites, unlike glass and other cellulose fibre-filled system[18,19]. For a given shear stress, viscosity of the composite increases with fibre loading. This is true for all shear stresses. In the low shear stress region, there would be little deformation, and strong interaction between fibres and polyethylene due to the agglomeration of fibres would result in a high viscosity. As the level of shear stress is increased, fibres will align along the direction of flow and consequently viscosity decreases.

Effect of fibre length

Figure 3 shows the effect of fibre length on the melt viscosity of PALF–LDPE composites. It can be noticed that the viscosity marginally increases upon the increase of fibre length from 2 to 10 mm. At higher fibre length the dispersion of fibre is not so good and at the same time difficult to orient in the direction of flow. This is associated with the fibre entanglement at higher fibre loading. Fibres having shorter length are more easily aligned and distributed along the direction of flow than longer fibres.

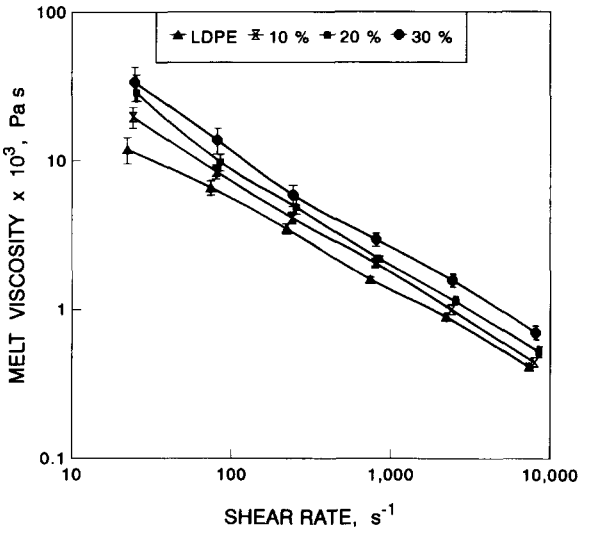

Figure 1 Variation of melt viscosity (η) with shear rate ($\dot{\gamma}$) of PALF–LDPE composites at a temperature of 125°C. Fibre length 6 mm

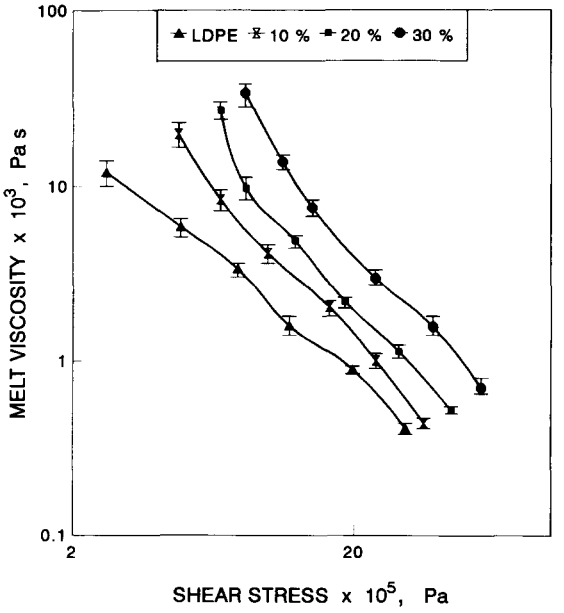

Figure 2 Variation of melt viscosity (η) with shear stress ($\dot{\gamma}$) of PALF-LDPE composites at a temperature of 125°C. Fibre length 6 mm

Effect of chemical treatments

Studies on the composite materials have shown that the bonding between the reinforcing fibre and the matrix has a significant effect on the properties of the composite. Good bonding at the interface can be achieved by modifying the fibre–matrix interface with various surface reactive additives or coupling agents[20–22]. In order to enhance the fibre–matrix interaction PALF was treated with various reagents. The effect of chemical treatments on viscosity of PALF–LDPE composite at a temperature of 125°C is shown in *Figure 4*. It is clear that the viscosity of the composite increases as a result of chemical treatment. Silane treatment enhances adhesion at the polymer–fibre interface, and in the process the viscosity is increased. The improved interface adhesion due to silane treatment can be explained in terms of a possible hypothetical structure in the interfacial area of PE and fibre (*Figure 5*). The general formula for silane coupling agents is $YR_1Si(OR_2)_3$. In this, Y is the polymerizable vinyl group in silane. During coating treatment, $-OR_2$ groups of silane may hydrolyse to some extent to form silanols:

$$YR_1Si(OR_2)_3 \xrightarrow{H_2O} YR_1Si(OH)_3 \qquad (6)$$

The resulting –OH group or $-OR_2$ group provides a link to cellulose through their –OH groups by the formation of hydrogen bonds. Dicumylperoxide, which is used as an initiator during coating treatment, helps to polymerize vinyl groups. Individual silane coupling agent molecules, which are supposed to attach to cellulose, form a continuous link. The long hydrophobic polymer chain of polymerized silane can adhere to PE due to van der Waal's type adhesive forces. As a result, a strong interaction is induced at the fibre–matrix interface and friction between the polymer and fibre is increased[23]. This results in an increase of viscosity. The tensile fracture surfaces of untreated and silane treated composites, given in *Figure 6*, indicate the strong fibre–matrix interaction. *Figure 6a* indicates fibre pull-out in untreated composite. The strong adhesion between fibre and matrix can be seen in *Figure 6b* where polyethylene fragments are sticking to the fibre surface.

The increase in viscosity in PMPPIC treated fibre composite is due to the increased interaction between fibre and matrix. The enhanced bonding is attributed to the formation of strong covalent bonds between –OH groups of cellulose present in PALF and –NCO group of PMPPIC. This was confirmed by the presence of carbonyl groups by i.r. studies. The –N=C=O group in PMPPIC is highly reactive to the –OH group of cellulose and therefore a urethane linkage is formed.

$$-N=C=O + HO-\text{cellulose} \rightarrow -\overset{H}{\underset{|}{N}}-\overset{O}{\overset{\|}{C}}-O-\text{cellulose} \qquad (7)$$

A possible hypothetical chemical structure in the interfacial area of the PMPPIC treated composite is

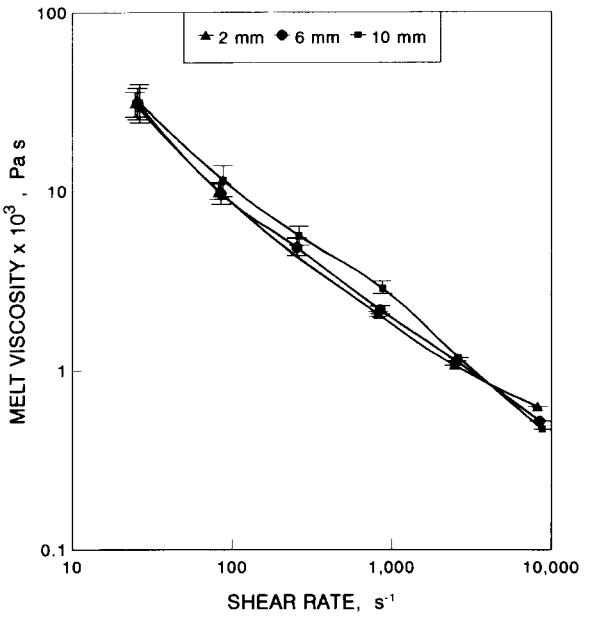

Figure 3 Variation of melt viscosity (η) with shear rate ($\dot{\gamma}$) at different fibre lengths at a temperature of 125°C

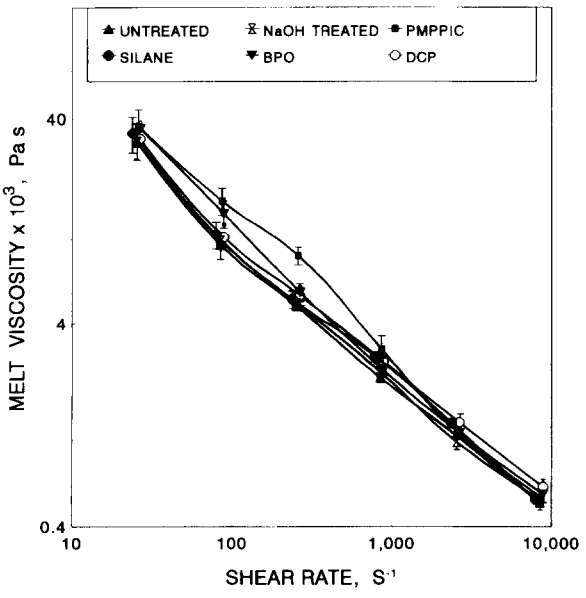

Figure 4 Variation of melt viscosity with shear rate of PALF–LDPE composites for different fibre treatments. Fibre length 6 mm and temperature 125°C

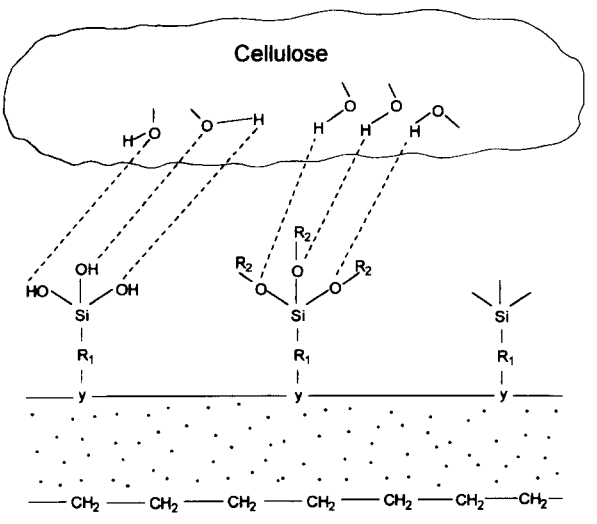

Figure 5 Hypothetical chemical structure of cellulose–silane–polyethylene in the interfacial area

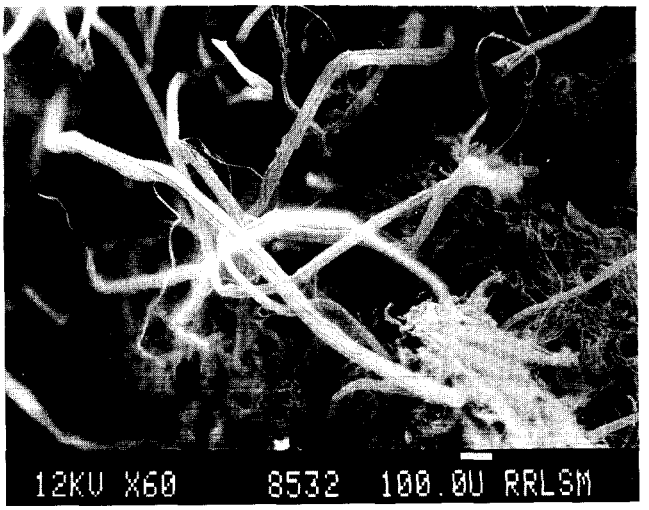

a

b

Figure 6 Scanning electron micrographs of tensile fracture surfaces of (a) untreated fibre composite indicating fibre pull-out, and (b) silane treated fibre composite; polyethylene fragments are sticking to the surface

shown in *Figure 7*. The long chain molecules present in PMPPIC interact with polyethylene leading to a Van der Waal's type of interaction. Thus, the increased frictional force exerted by the treatment results in the increase of viscosity. Also, decreased hydrophilicity of the fibre due to the isocyanate treatment (confirmed by equilibrium swelling) makes the system more compatible with the hydrophobic polyethylene matrix. This may also lead to an increase in viscosity. The better fibre–matrix adhesion of composite is evident from scanning electron micrographs given in *Figures 8a* and *b*. The treated fibres adhere well to the polymer matrix. The peroxide treated composites also show higher viscosity than the untreated composites. This is due to the fact that during processing in the presence of peroxides, grafting of polyethylene on to cellulose fibres occurs by combining cellulose and polyethylene radicals. This is a free radical initiated reaction as shown below:

$$RO{-}OR \rightarrow 2RO^{\cdot} \quad (8)$$

$$RO^{\cdot} + PE{-}H \rightarrow ROH + PE^{\cdot} \quad (9)$$

$$RO^{\cdot} + \text{cellulose}{-}H \rightarrow ROH + \text{cellulose}^{\cdot} \quad (10)$$

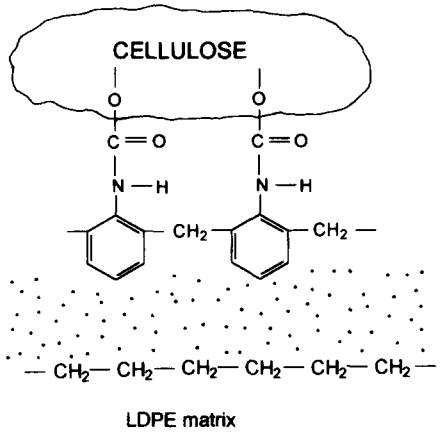

Figure 7 Hypothetical chemical structure of cellulose–PMPPIC–polyethylene in the interfacial area

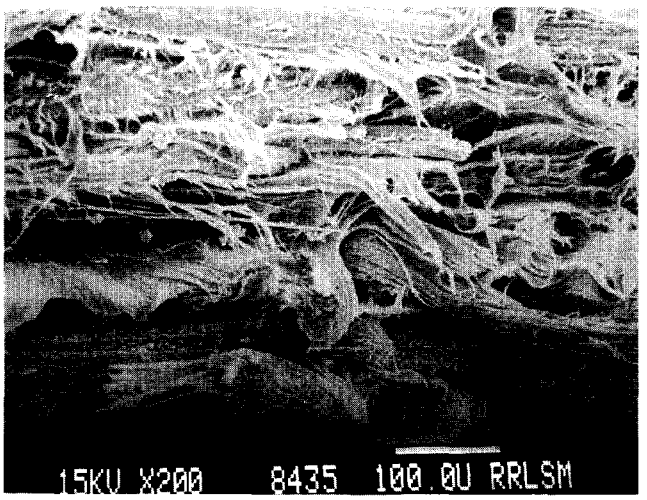

a

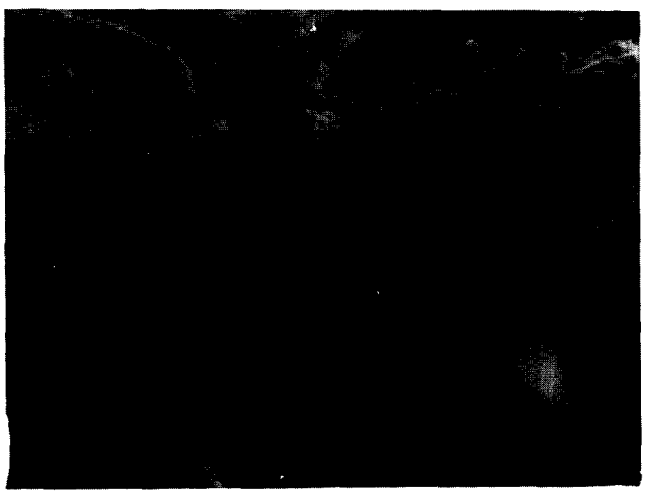

b

Figure 8 (a,b) Scanning electron micrographs of tensile fracture surfaces of PMPPIC treated composite

$$PE^{\cdot} + \text{cellulose}^{\cdot} \rightarrow PE{-}\text{cellulose} \quad (11)$$

The efficiency of these reactions increases with peroxide concentration.

Other reactions possible during the processing of composite are an increase of molecular weight and cross-linking of polymer matrix by combining polyethylene

radicals[24]. All these lead to the increase in melt viscosity:

$$PE^{\cdot} + PE^{\cdot} \rightarrow PE-PE \quad (12)$$

The better interaction between fibre and matrix in the peroxide treated composite can be understood from the tensile failure surface of peroxide treated composite (*Figure 9*). It can be seen that the polyethylene is grafted to the fibre surface.

The increase in viscosity in NaOH treated composite is attributed to the increased mechanical interlocking between fibre and matrix. During alkali treatment the fibre surface becomes rough due to the removal of waxy material present on the surface. The rough surface topography provides better mechanical interlocking with the polyethylene matrix.

Effect of temperature

Substantial temperature changes occur at various stages during moulding and it is important to study the effect of temperature on viscosity. In the present study, flow curves were made at 125, 135 and 145°C. *Figure 10* shows the variation of viscosity with temperature at different fibre loading at two shear rates. It is clear that viscosity decreases with increase of temperature for the filled and unfilled systems. At higher temperature, the molecular motion is accelerated due to the availability of greater free volume and also due to decreasing entanglement density and weaker intermolecular interactions. The decrease in viscosity is more predominant at low shear rate than at high shear rate. This may be due to the high residence time of the melt in the barrel of the capillary rheometer at low shear rate.

To further understand the influence of temperature on the viscosity of composites, Arrhenius plots at constant shear rate were made (*Figure 11*). In this figure the logarithm of viscosity is plotted against reciprocal temperature. Linear plots were obtained. The activation energy of a material provides valuable information on the sensitivity of material toward the changes in temperatures. The higher the activation energy the more temperature sensitive the material will be. The activation energies of the system at different fibre loading are given in *Table 1*. The flow of composite is dependent on the quantity of fibre present in the system as well as on temperature and shear rate, i.e. the presence of fibre restricts molecular motion.

In the case of composites containing treated fibre a different trend is observed (*Tables 2* and *3*). There is an

Figure 9 Scanning electron micrographs of tensile fracture surfaces of BPO treated PALF–LDPE composite: polyethylene is grafted on the fibre surface

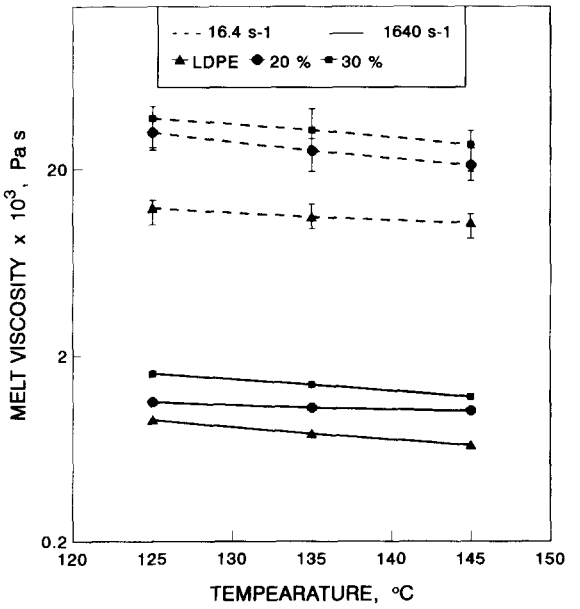

Figure 10 Variation of melt viscosity (η) with temperature at different shear rates and at different fibre loading. Fibre length 6 mm

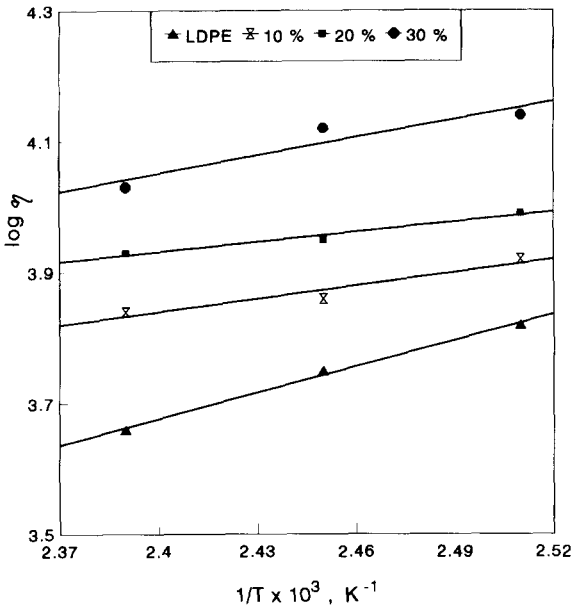

Figure 11 Plot of $\log \eta$ *versus* $1/T$

Table 1 Activation energy of PALF–LDPE composites at different fibre loading

System	Activation energy (cal)
LDPE	792
LDPE + 10 wt% fibre	397
LDPE + 20 wt% fibre	298
LDPE + 30 wt% fibre	546

Table 2 Viscosity of untreated and treated composites at various temperatures

Shear rate (s^{-1})	Viscosity (Pa s)					
	Untreated		Isocyanate		Silane	
	125°C	135°C	125°C	135°C	125°C	135°C
22.2	3.5×10^4	2.53×10^4	3.69×10^4	4.44×10^4	3.40×10^4	2.59×10^4
84	9.71×10^3	8.82×10^3	1.59×10^4	1.48×10^4	1.09×10^4	9.08×10^3
222	4.85×10^3	4.30×10^3	8.60×10^3	6.32×10^3	5.26×10^3	4.33×10^3
840	2.18×10^3	2.14×10^3	3.00×10^3	2.95×10^3	2.77×10^3	2.59×10^3
2222	1.13×10^3	1.10×10^3	1.57×10^3	1.17×10^3	1.30×10^3	1.12×10^3
8400	5.22×10^2	5.00×10^2	7.00×10^2	5.59×10^2	5.70×10^2	5.45×10^2

Table 3 Viscosity of peroxide treated composites at various temperatures

Shear rate (s^{-1})	Viscosity (Pa s)			
	BPO		DCP	
	125°C	135°C	125°C	135°C
22.2	3.60×10^4	3.76×10^4	3.2×10^4	3.35×10^4
84	1.38×10^4	1.68×10^4	1.06×10^4	1.17×10^4
222	5.69×10^3	6.19×10^3	5.47×10^3	6.39×10^3
840	2.38×10^3	2.65×10^3	2.63×10^3	2.62×10^3
2222	1.38×10^3	1.16×10^3	1.27×10^3	1.12×10^3
8400	7.49×10^2	5.80×10^2	6.30×10^2	5.26×10^2

increase of viscosity of composites when the temperature is increased from 125 to 135°C. This behaviour is exhibited by isocyanate treated and peroxide treated fibre composites at low shear rates. But at high shear rates this difference is less because the residence time of melt in the barrel is less.

At higher temperature, crosslinking is expected to take place during extrusion. In order to analyse the extent of crosslinking, the crosslink density of the composites was determined by equilibrium swelling method using the equation[25].

$$M_c = \frac{-\rho_c V(\phi)^{1/3}}{\ln(1-\phi) + \phi + \chi\phi^2} \tag{13}$$

where ρ_c = density of composite, V = molar volume of solvent and ϕ = volume fraction of polymer in the solvent swollen sample which is given by

$$\phi = \frac{d - (fw)\rho_c^{-1}}{[d - (fw)]\rho_c^{-1} + A_0\rho_s^{-1}} \tag{14}$$

where w = weight of sample, d = weight after drying the sample, f = fraction of insoluble component and A_0 = weight of solvent. The interaction parameter χ is given by

$$\chi = \beta + (V_s/RT)(\rho_s - \rho_c)^2 \tag{15}$$

where β = lattice constant (0.34), V_s = molar volume of solvent, R = gas constant, T = temperature, ρ_s = solubility parameter of solvent and ρ_c = solubility parameter of the composite. As the effective bonding between the matrix and fibre increases the restriction to swelling increases. The degree of crosslinks (γ) has been determined from M_c values as $1/2M_c$. The differences in crosslink density values of composites at two different temperatures are shown in *Table 4*. It is clear that the crosslink density of peroxide treated composite is higher at 135°C. Therefore it can be concluded that the increase in viscosity of the composite with temperature is due to the increased crosslink density of the system.

Table 4 Crosslink density values of composites at two different temperatures

Composite	Crosslink density	
	125°C	135°C
PMPPIC treated	1.08×10^{-4}	1.40×10^{-4}
BPO treated	1.00×10^{-4}	1.35×10^{-4}
DCP treated	9.40×10^{-5}	1.20×10^{-4}

Shear stress–temperature superposition master curve

The application of shear rate–temperature superposition in predicting melt viscosities was reported by Anand[26]. The values of superposition shift factors were obtained by choosing a shear stress value at the reference temperature of 135°C and shifting the corresponding points on the flow curves for other temperatures to coincide with these shear stresses. The values of a_T were calculated from the following equation:

$$a_T = \frac{\tau(\text{ref})}{\tau_{(T)(\text{constant}\dot{\gamma})}} \tag{16}$$

The master curve is constructed by plotting the product $\tau_T a_T$ *versus* $\dot{\gamma}$ (*Figure 12*). It is clear that the curves at different temperatures shift to a single reference temperature curve. The superposition of the data was achieved over the whole range of temperature and shear rate. The average shift values for a reference temperature of 135°C are shown in *Figure 13* as $\log a_T$ *versus* $1/T$.

Comparison with theoretical prediction

For non-spherical particles Guth[27] proposed an equation to predict the viscosity of oriented composites:

$$\eta_c = \eta_{un}(1 + 0.6fc + 1.62f^2c^2) \tag{17}$$

where f = ratio of longest to shortest diameter of fibre, c = volume fraction of fibre, η_{un} = viscosity of unfilled system and η_c = viscosity of composite.

The theoretical and experimental viscosities of PALF filled polyethylene composites are shown in *Figure 14*. It is clear that experimental viscosity is higher than theoretical viscosity. This is associated with the misalignment of fibres as well as the fibre orientation distribution as explained earlier.

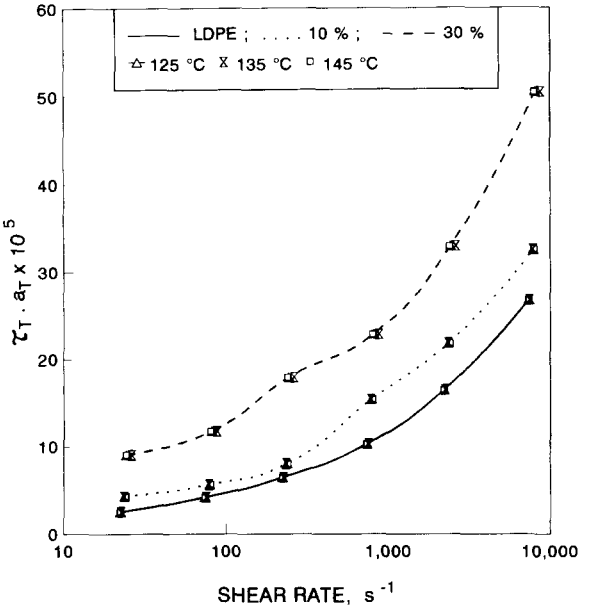

Figure 12 Shear stress *versus* temperature superposition master curves at different fibre loading

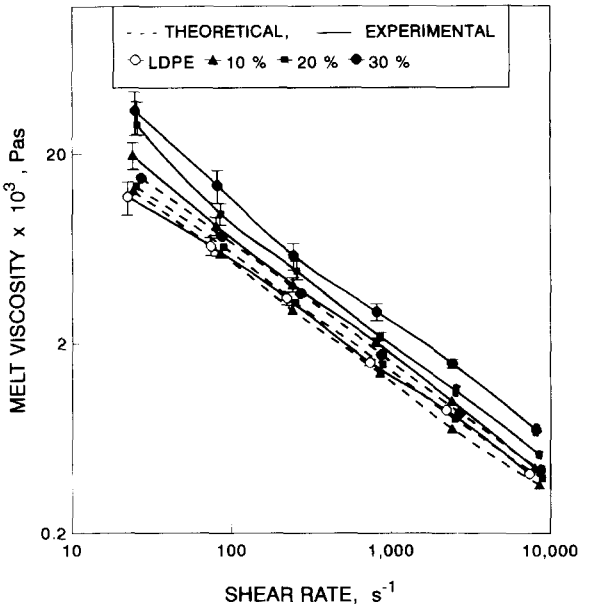

Figure 14 Comparison of theoretical and experimental viscosity at different fibre loading

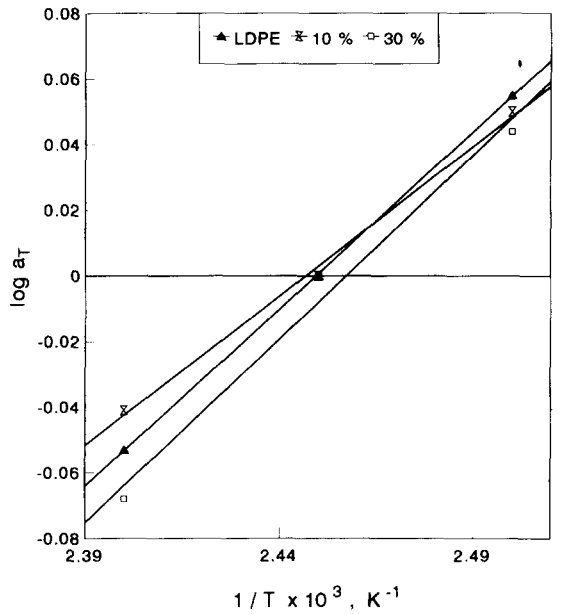

Figure 13 Plot of log a_T *versus* $1/T$

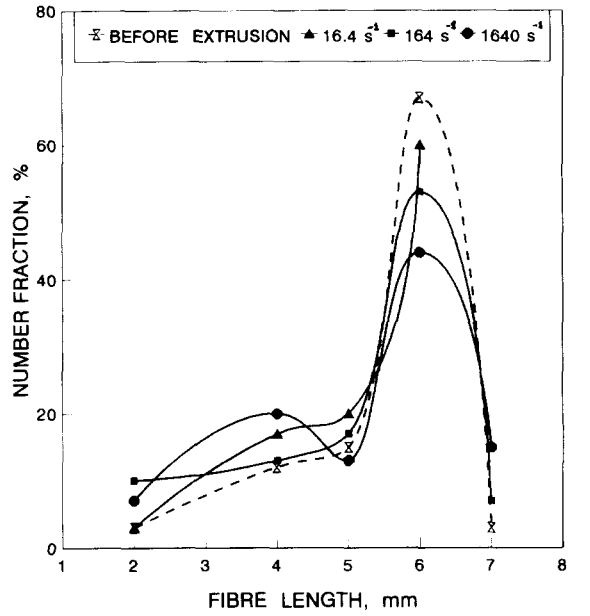

Figure 15 Plot of number fraction (%) *versus* fibre length

Fibre breakage analysis

The fibre length distribution of composites before and after extrusion through the capillary at three different shear rates is given in *Figure 15*. Owing to the high shear stresses during extrusion there is a possibility of fibre breakage. From the figure it is clear that about 70% of fibres retain the original length (6 mm) after extrusion through the injection moulding machine (nozzle diameter 4 mm). During extrusion at high shear rates, the fibre undergoes breakage. About 40% of fibres are of 3 mm length at a shear rate of 1640 s^{-1}. However, at all shear rates the most probable length is 6 mm. It is interesting to note that this value decreases linearly with increase of shear rate (*Figure 16*). This is associated with the breakage of fibres at high shear rates. The fibre length distribution can also be represented in the same way as molecular weight distribution. The number and weight averages are represented as:

$$\bar{L}_n = \frac{\sum NiLi}{\sum Ni} \tag{18}$$

$$\bar{L}_w = \frac{\sum NiLi^2}{\sum NiLi} \tag{19}$$

where $\bar{L}_n$ = number average fibre length, $\bar{L}_w$ = weight average fibre length and Ni = number of fibres having length Li. The ratio, $\bar{L}_w/\bar{L}_n$, the polydispersity index is taken as a measure of fibre length distribution. The fibre length distribution becomes broader as the value $\bar{L}_w/\bar{L}_n$ increases. The values of $\bar{L}_n$, $\bar{L}_w$ and $\bar{L}_w/\bar{L}_n$ based on 150 fibres extracted from the composites before and after extrusion are given in *Table 5*. The polydispersity index

remains the same before and after extrusion at all shear rate values.

Extrudate morphology

Figures 17a–c show the cross-section of extrudate containing 20% fibre at shear rates of 16.4 and 164 and 1640 s^{-1} respectively. The fibres which are concentrated at the periphery at low shear rate (*Figure 17a*) are dispersed uniformly at medium shear rate (*Figure 17b*). However, at high shear rate fibres are aligned along the direction of flow and concentrated at the core region (*Figure 17c*). *Figures 18a* and *b* show the surface morphology of the extrudates at different shear rates. It is clear from these figures that surface discontinuity increases with shear rates. Most of the extrudates have smooth surfaces and are of uniform diameter at low shear rates. But at high shear rates the extrudates exhibit surface irregularity.

Flow behaviour index

The effects of fibre loading and temperature on the flow behaviour index (n') are shown in *Table 6*. For all the systems, n' values are less than unity, characteristic of the pseudoplastic nature of the composites. The degree of pseudoplasticity of the composites increases with fibre loading and with temperature. The high pseudoplasticity arises due to the orientation of fibres. The flow behaviour index of treated fibre composites at 20% fibre loading is given in *Table 7*. The pseudoplasticity of

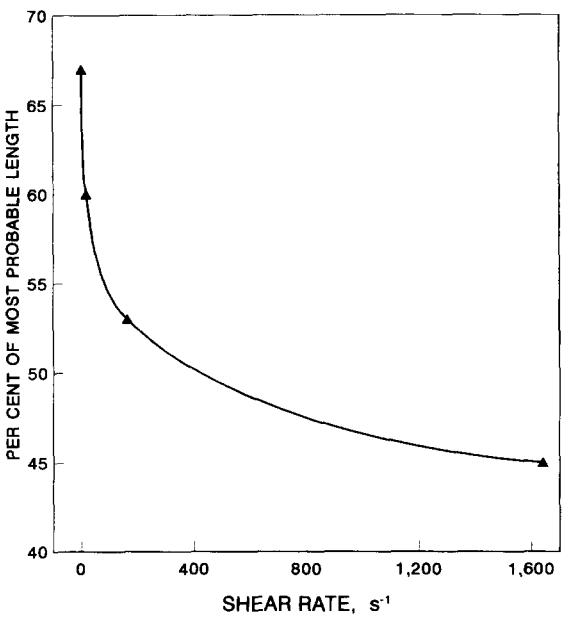

Figure 16 Plot of most probable length *versus* shear rate ($\dot{\gamma}$)

Table 5 Fibre length distribution index

Fibre	$\bar{L}_n$	$\bar{L}_w$	$\bar{L}_w/\bar{L}_n$
Before extrusion	5.53	5.68	1.027
After extrusion at shear rate of			
16.4 s^{-1}	4.33	5.51	1.034
164 s^{-1}	5.33	5.56	1.04
1640 s^{-1}	4.73	5.14	1.086

Table 6 Flow behaviour index (n') of composite at different fibre loading

	n'		
System	125°C	135°C	145°C
LDPE	0.417	0.403	0.414
PE + 10% fibre	0.355	0.346	0.341
PE + 20% fibre	0.314	0.300	0.299
PE + 30% fibre	0.294	0.290	0.289

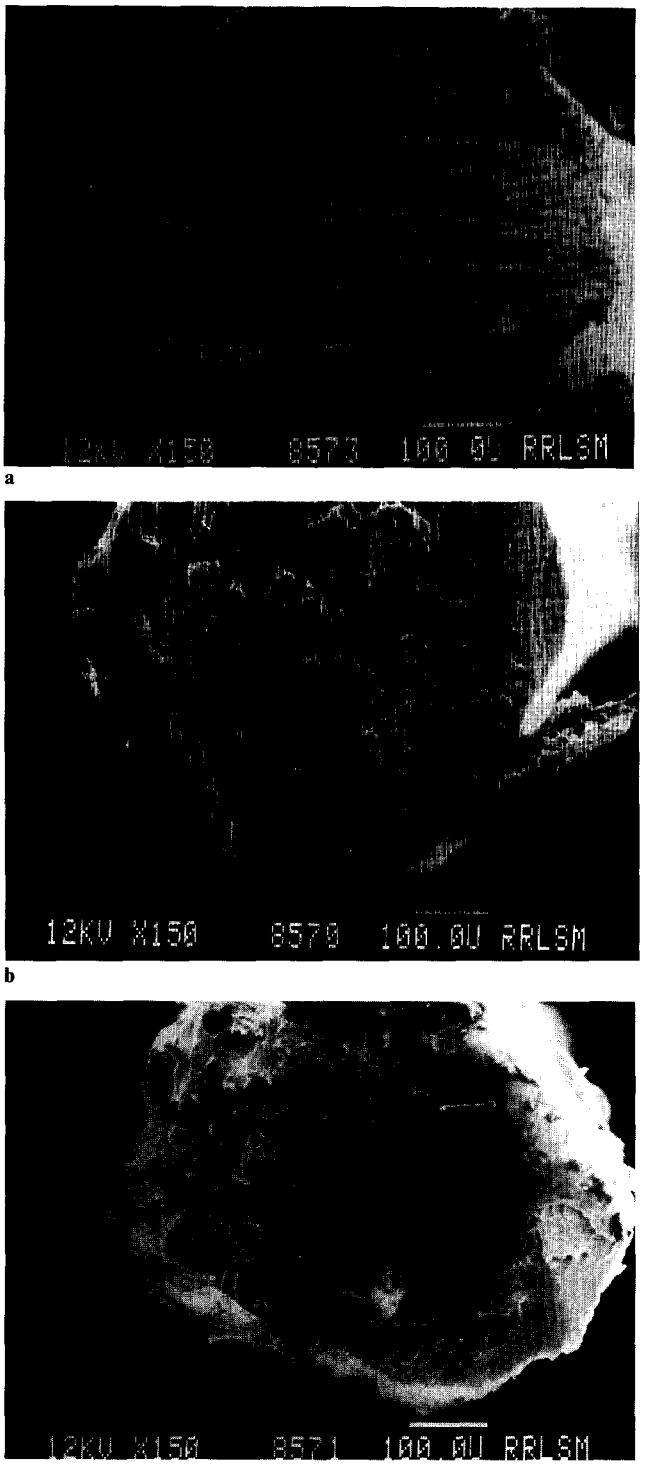

Figure 17 Scanning electron micrographs of cross-section of extrudate at different shear rates: (a) 16.4 s^{-1} (fibres are concentrated at the periphery); (b) 164 s^{-1} (fibres are uniformly dispersed); (c) 1640 s^{-1} (fibres are concentrated at the core region)

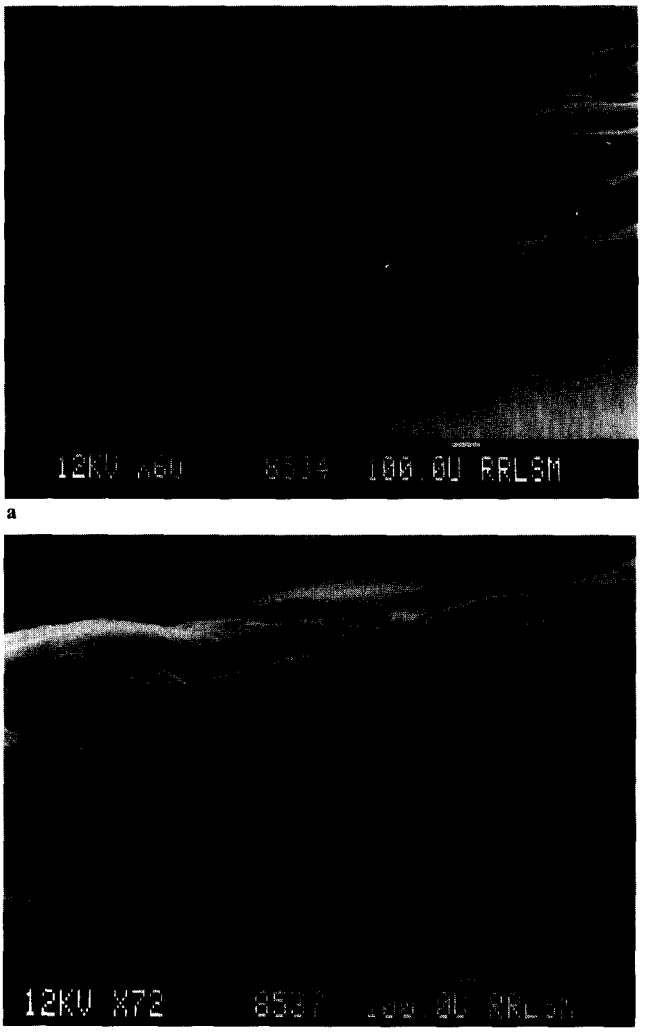

a

b

Figure 18 Scanning electron micrographs of the surface morphology of extrudate at different shear rates: (a) 16.4 s^{-1}; (b) 1640 s^{-1}

Table 7 Flow behaviour index (n') of treated fibre composites: fibre loading 20 wt%

	n'		
Treatment	125°C	135°C	145°C
Untreated	0.314	0.300	0.299
PMPPIC	0.287	0.258	0.226
Silane	0.312	0.355	0.363
BPO	0.281	0.288	0.299
DCP	0.288	0.290	0.284

treated composites is higher than that of untreated composites except in the case of silane treated composite.

Correlation between melt flow index and capillary rheometer data

Although MFI may be a good indicator for studying the effect of processing history of the polymer, it cannot correlate directly with processing behaviour since the values of temperature and shear rate employed in the MFI test differ substantially from those encountered in the actual process. Shenoy *et al.*[28,29] developed a method to estimate the rheograms from a knowledge of MFI for polyolefins, styrenics and cellulosics. Bhagawan *et al.*[30]

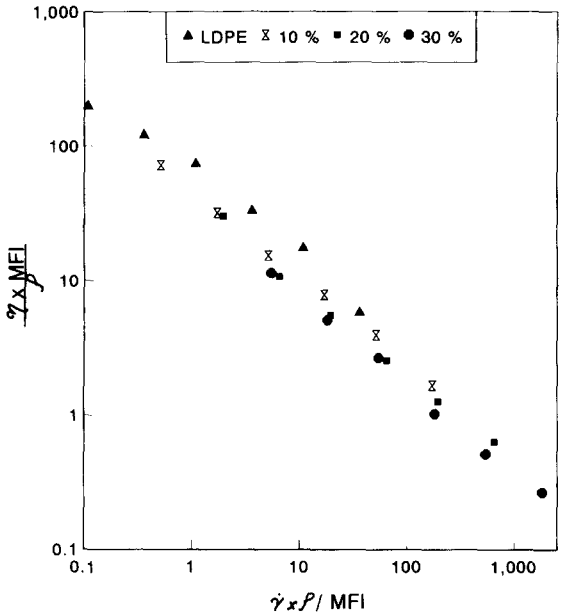

Figure 19 Viscosity master curves for different PALF–LDPE systems at 145°C

Table 8 MFI values of PALF–LDPE composites (g/10 min) at 145°C

System	MFI
LDPE	180
10% fibre	43.71
20% fibre	12.27
30% fibre	4.542

combined the MFI data and capillary rheometer data to provide master curves for silica and black filled thermoplastic 1,2-polybutadiene rubber.

Figure 19 shows the master curve of composite obtained by correlating MFI (*Table 8*) and capillary rheometer data at different fibre loading. Using a plot of $\eta \times \text{MFI}/\rho$ *versus* $\dot{\gamma} \times \rho/\text{MFI}$ (ρ = density of composite), it is shown that the four curves were unified as a single curve. The advantage of such a master curve is that simple evaluation of MFI would be adequate to generate viscosity *versus* shear rate curves without the use of sophisticated rheological instruments.

CONCLUSION

Melt rheological properties of short pineapple fibre reinforced low density polyethylene composites have been studied as a function of fibre loading, fibre length, shear rate and temperature. In general the viscosity of the system increased with fibre loading due to an increased hindrance to the flow. The influence of chemical treatments on the melt flow properties was studied. It is found that addition of bonding agents increases the viscosity of composite due to the increased fibre–matrix interaction. The melt flow studies were carried out in the temperature range of 125 to 145°C and activation energy of the system was calculated using the Arrhenius equation. It was found that viscosity of the melt decreases with increase of temperature. This is associated with the molecular motion due to the availability of greater free volume and weaker intermolecular interactions. However, the treated composites showed an opposite trend

due to the crosslinking of composite at higher temperature. The extent of crosslinking was analysed by determining the crosslink density of the composites by the equilibrium swelling method. Using an arbitrary reference temperature a superposition method was found to be applicable over the entire region of shear stress–temperatures. Flow curves at various temperatures were found to be superimposable by the application of this method. A comparison is made between theoretical and experimental viscosity values and it is found that experimental viscosity is slightly higher than theoretical viscosity because of the misalignment of fibres. Fibre breakage analysis was carried out to study the fibre distribution. It was found that the percentage of most probable length decreases linearly with increasing shear rate. Cross-sectional and surface morphology of the extrudates were analysed by optical and scanning electron microscopies. It was observed that the fibres which were concentrated at the periphery at low shear rate were well dispersed at medium shear rate and migrated to the core region at very high shear rate. MFI of the composites was measured and master curves were generated using modified viscosity and shear rate function with MFI as one of the parameters.

ACKNOWLEDGEMENTS

One of the authors (J. G.) is thankful to the Council of Scientific and Industrial Research, New Delhi, for financial support. Thanks are also due to Dr K. Ramamurthy, Deputy Director, CIPET, Madras, for permission and Mr Murukesan for technical assistance for the completion of the work.

REFERENCES

1 Fujiyama, M. and Kawasaki, J. *J. Appl. Polym. Sci.* 1991, **42,** 481
2 Wang, K. J. and Lee, L. J. *J. Appl. Polym. Sci.* 1987, **33,** 431
3 Crown, J., Folkes, M. J. and Bright, P. F. *Polym. Eng. Sci.* 1980, **20,** 925
4 Brydson, J. A. 'Flow Properties of Polymer Melts', 2nd edn, George Godwin, London, 1981
5 Gupta, A. K. and Purwar, S. N. *J. Appl. Polym. Sci.* 1985, **30,** 1777
6 Molden, G. F. *J. Mater. Sci.* 1969, **4,** 283
7 Crowson, R. J., Folkes, M. J. and Bright, P. F. *Polym. Eng. Sci.* 1980, **20,** 63
8 Crowson, R. J. and Folkes, M. J. *Polym. Eng. Sci.* 1980, **20,** 934
9 Murthy, V. M., Gupta, B. R. and De, S. K. *Plast. Rubber Process. Appl.* 1985, **5,** 307
10 Varghese, S., Kuriakose, B., Thomas, S., Premaletha, C. K. and Koshy, A. T. *Plast. Rubber Comp. Process. Appl.* 1993, **20,** 93
11 Joseph, K., Kuriakose, B., Thomas, S. and Premalatha, C. K. *Plast. Rubber Comp. Process. Appl.* 1994, **21,** 238
12 George, J., Joseph, K., Bhagawan, S. S. and Thomas, S. *Mater. Lett.* 1993, **18,** 161
13 George, J., Prabhakaran, N., Bhagawan, S. S. and Thomas, S. *J. Appl. Polym. Sci.* 1995, **57,** 843
14 George, J., Bhagawan, S. S. and Thomas, S. *J. Thermal Analysis* in press
15 Bagley, E. B. *Trans. Soc. Rheol.* 1961, **5,** 355
16 Goldsmith, H. L. and Mason, S. G. in 'Rheology Theory and Application' (Ed. F. R. Eirich), Vol. 4, Academic Press, New York, 1967
17 Wu, S. *Polym. Eng. Sci.* 1979, **19,** 638
18 Tanaka, H. and White, J. L. *Polym. Eng. Sci.* 1980, **20,** 949
19 White, J. L., Zarnecki, L. and Tanaka, H. *Rubber Chem. Technol.* 1980, **53,** 823
20 Raj, R. G., Kokta, B. V., Groukau, G. and Daneault, C. *Polym. Plast. Technol. Eng.* 1990, **29,** 339
21 Maldas, D., Kokta, B. V. and Deneault, C. J. *Appl. Polym. Sci.* 1989, **37,** 751
22 Raj, R. G., Kokta, B. V. and Daneault, C. J. *Adhesion Sci. Technol.* 1989 **3,** 55
23 Erickson, P. W. 25th Annual Technical Conference SPI, 13-A, 1917
24 Sapieha, S., Allard, P. and Zang, Y. H. *J. Appl. Polym. Sci.* 1990, **41,** 2039
25 Flory, P. J. and Rehner, J. *J. Chem. Phys.* 1943, **11,** 521
26 Anand, J. S. *Int. Plast. Eng. Technol.* 1994, **1,** 25
27 Guth, E. *J. Appl. Phys.* 1945, **16,** 20
28 Shenoy, A. V., Saini, D. R. and Nadkarni, V. M. *J. Appl. Polym. Sci.* 1982, **27,** 4399
29 Shenoy, A. V., Saini, D. R. and Nadkarni, V. M. *Polym. Eng. Sci.* 1983, **28,** 722
30 Bhagawan, S. S., Tripathy, D. K., De, S. K., Sharma, S. K. and Ramamurthy, K. *Polym. Eng. Sci.* 1988, **28,** 648